Journal of Applied Polymer Science

A Comparative Study on Curing Characteristics and Thermomechanical Properties of Elastomeric Nanocomposites: The Effects of Eggshell and Calcium Carbonate Nanofillers

Mohammad Reza Saeb,[1] Hadi Ramezani-Dakhel,[2] Hossein Ali Khonakdar,[3] Gert Heinrich,[4,5] Udo Wagenknecht[4]

[1]Department of Resin and Additives, Institute for Color Science and Technology, Tehran 16765-654, Iran
[2]Department of Polymer Engineering, College of Polymer Science and Polymer Engineering, University of Akron, Akron, Ohio 44325-0301
[3]Department of Polymer Processing, Iran Polymer and Petrochemical Institute, Tehran 14965-115, Iran
[4]Department of Materials and Processing, Leibniz-Institut für Polymerforschung Dresden e. V., Hohe Strasse 6, Dresden D-01069, Germany
[5]Department of Mechanical Engineering, Technische Universität Dresden, Institut für Werkstoffwissenschaft, Dresden D-01069, Germany
Correspondence to: H. Ramezani-Dakhel (E-mail: hr15@zips.uakron.edu)

ABSTRACT: After-hatching eggshell (AHES) nanobiofiller and nanocalcium carbonate (nano-CA) were separately added to various elastomers, such as acrylonitrile butadiene rubber (NBR), styrene butadiene rubber (SBR), and natural rubber (NR), in various amounts of 5, 10, and 15 phr. The effect of particle size and dispersion of such nanofillers on thermomechanical properties and curing characteristics were then investigated. The ultimate tensile properties of SBR and NR nanocomposites were improved to some extent when 5 phr of AHES nanofiller was added to the rubber compound compared to CA. In the case of NBR nanocompounds, however, the mechanical properties were seemingly comparable, irrespective of the type of nanofiller. This contradictive behavior could be attributed to the alteration of crosslink density due to particular filler–matrix interaction while using mineral and natural fillers. The results of the rheometric study revealed that using AHES rather than CA slightly increases the scorch time of all types of prepared nanocomposites, whereas a significant drop in the optimum curing time was seen for NBR nanocomposites containing AHES biofiller. Moreover, thermogravimetric analysis showed similar thermal stability for SBR nanocomposites containing AHES and CA fillers. Finer particle size of CA and higher porosity of AHES at high and low loading levels were respectively the main reasons for improvement of ultimate properties. © 2012 Wiley Periodicals, Inc. J. Appl. Polym. Sci. 000: 000–000, 2012

KEYWORDS: elastomeric nanocomposites; eggshell; calcium carbonate; curing; mechanical properties

Received 13 December 2011; accepted 6 May 2012; published online
DOI: 10.1002/app.38022

INTRODUCTION

Natural rubber (NR), acrylonitrile butadiene rubber (NBR), and styrene butadiene rubber (SBR) have attained substantial interests for tires, inner tubes, automotive parts, agricultural equipments, and other industrial facilities.[1] Regardless of the nature of these materials (polarity effects), the lack of reinforcing agents, for example, carbon black and silica fillers in rubber compound, leads to improper properties. The performance of filler intensely depends on its physical interaction with the matrix component. Among different types of inorganic fillers, calcium carbonate (CA) is widely used in elastomeric compounds because of its performance at high loading levels. Several researchers have already prepared polymer nanocomposites using the micron-sized and nanosized CA inorganic filler.[2–12] To avoid agglomeration, especially when CA nanofiller is used, the surface energy resulting from filler–filler interactions needs to be lowered via coating the filler surface with carboxylic monomers like stearic acid.[2,3,6,10]

The nanosized CA has occasionally been used to prepare elastomeric nanocomposites with satisfactory thermal and mechanical properties.[4–7,9,11,12] Jin and Park[4] have demonstrated that the thermal stability and mechanical properties of the butadiene rubber/CA (40–70 nm) composites were considerably improved

when an optimum level of filler (15 wt %) was used. Likewise, Mishra et al.[5] inferred that when the size of nano-CA lowers from 21 to 9 nm, the thermomechanical properties of SBR compounds improve considerably due to superior dispersion of fine nanofillers. They also showed that the best properties can be achieved at 8 wt % of filler, irrespective of filler size.

Lipińska et al.[10] prepared surface-modified nanosized CA particles and incorporated the coated filler with NBR and EPR elastomers. They declared that because of the porosity effect of the used filler, the free energy on the filler surface was significantly reduced. Hence, the crosslink density of rubber network was increased after modification of filler surface. However, the results dealt with vulcanizates containing unsaturated acids were quite different. Osman et al.[2] reported that using stearic acid as surface modifier results in linear increment of modulus and yield stress in LDPE/CA composites containing uncoated fillers. On the other hand, tensile strength, yield strain, and elongation at break were decreased after surface treatment with stearic acid. Nonetheless, overcoating of the filler surface cannot guarantee the linear superposition of the effects, and therefore, the influence of excessive surfactant on the composite properties cannot be simply predicted. In other words, an optimal amount of surfactant ought to be used to guarantee proper monolayer coating.

In that case, using nanofillers can regulate some ultimate properties depending on the filler shape, particle size, aggregate size, and surface characteristics of the matrix. Eggshell is a byproduct of incubation farms, and there is an ever-increasing demand for developing suitable methods for disposal of this matter. To our knowledge, only a few studies have been focused on using eggshell powder as filler for polymer matrices. So far, eggshell wastes have incorporated with polypropylene[13] and poly(vinyl chloride)[14] matrices as well as poly(styrene-*b*-ethylene/butylene-*b*-styrene) biodegradable composites.[15] Moreover, there are limited works that have dealt with elastomeric matrices reinforced with eggshell powder.[16,17] As the most part of eggshell contains more than 90% of CA, one can imagine comparable consequences while using eggshell and CA fillers. Nevertheless, it has been found that[16,17] during incubation period, embryo nurtures from the innermost mammillary layer of eggshell and a porous structure forms. Surprisingly, these porosities exist even after trituration by planetary mill. This fact reasons enhanced properties of NR, NBR, and SBR nanocomposites incorporated with micron-sized eggshell powders when compared with those with CA.[17] Among two types of eggshell powders, after-hatching eggshell (AHES) and before-hatching eggshell (BHES), the former resulted in substantial improvements when compared with BHES and also CA nanofillers.

This work is an attempt to study the influence of surface-modified nano-CA and hatched eggshell biofiller (AHES) on ultimate properties of NR, NBR, and SBR nanocompounds. The triturated AHES was first coated with stearic acid to modify its surface toward elastomeric nanocomposites. Then, curing characteristics and thermomechanical properties were precisely considered for both unfilled and filled formulations. Scanning electron microscope (SEM) was used to study the dispersion of the used fillers in elastomeric nanocomposites.

Table I. Specifications of the Used Elastomers

Rubber	Commercial grade	Mooney viscosity[a]	Manufacturer
NR	SMR20	65	TEH AH YAU Rubber Factory, Semeling, Malaysia
SBR[b]	1502	53	Bandar Imam Petrochemical Co., Mahshahr, Iran.
NBR	KNB35L	41	Kumho Petrochemical Co., Ltd., Seoul, Korea

[a]Mooney viscosity (ML 1 + 4, 100°C), [b]This grade of SBR contains 23.5% styrene.

EXPERIMENTAL

Materials

Typical specifications of the used elastomers are reported in Table I. The basic materials used in compounds are as follows: sulfur (purity 99.8%), paraffin wax (MW = 352, density = 0.91 g/cm^3), stearic acid (MW = 284.5, density = 0.85 g/cm^3), and zinc oxide (MW = 81.4, density = 5.6 g/cm^3) (all provided from Razi and Bandar Imam companies, Mahshahr, Iran). Two accelerators are simultaneously used while compounding, tetramethylthiuram disulfide (TMTD) with melting point of 148°C and density of 1.43 g/cm^3 and dibenzothiazyl disulfide (MBTS) with melting point of 166°C and density of 1 g/cm^3. The former is purchased from Akrochem Corporation, and the latter from Meyors, China Chemical. The stearic acid-coated nanoprecipitated CA (NPCCA-201) is provided from Shandong Haize Nanomaterials, Shanghai, China. This filler has a cubic shape with an average particle size of about 50 nm, according to the supplier. AHES is purchased from a local company. The eggshell composition is as follows: CA 93.7%, organic part 4.14%, magnesium carbonate 1.39%, phosphate 0.73%, and 0.04% moisture. The organic part mostly contains I, V, and X types of collagen.[16,17] The AHES is first washed and dried and then triturated using a planetary mill for 6 h. Eventually, the prepared powder is dried at 80°C overnight. The particle size and geometrical shape of CA and AHES fillers are roughly compared in Figure 1. The average particle size and specific surface area of both types of fillers are also compared in Table II.

Sample Preparation

Surface Modification of Eggshell Particles. The CA nanofiller used in this work is coated by stearic acid as received. To compare the characteristics of nanocomposites containing AHES with those prepared using CA, a procedure is used to modify the surface of eggshell particles with stearic acid. Accordingly, a certain amount of stearic acid (8 wt %) dissolved in toluene and then eggshell powder is added to the mixture while stirring at room temperature overnight until equilibrium is reached. Eventually, coated powders are washed, filtered, and then dried at 80°C overnight.

Preparation of Elastomeric Nanocomposites and Characterization. Irrespective of the type of elastomers, compounding formulation for each unfilled rubber is given in Table III. In case of filled compounds, the contents of CA and AHES nanofillers were separately varied from 5 to 15 phr. The mixing

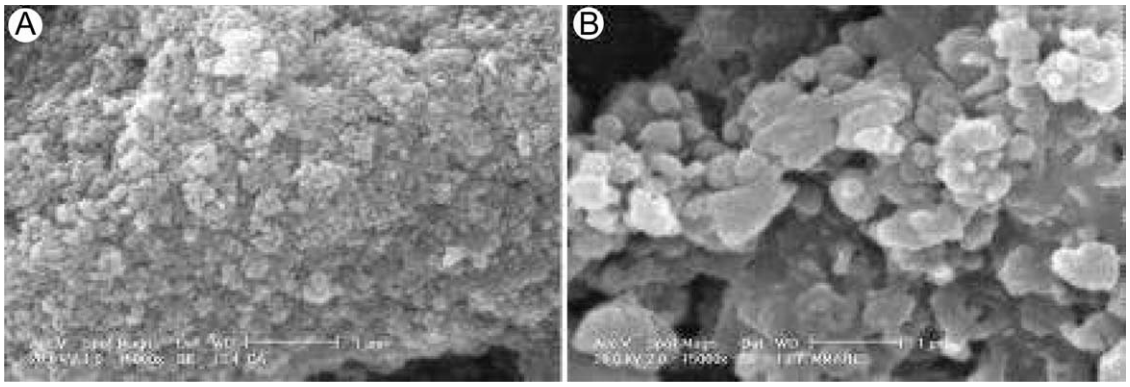

Figure 1. SEM micrographs of (A) CA and (B) AHES fillers.

of rubber, zinc oxide, TMTD antioxidant, and stearic acid was carried out using a laboratory open two-roll mill at 60°C for 5 min. The gear friction of the mill was 1 : 1.2. Furthermore, the filler was added to the compound and milled at 60°C for 10 min. The prepared sheets, of about 2 mm in thickness, were vulcanized at 160°C and 70 bars by using a hydraulic press. Hereafter, the A/B/C compound is briefly representative for the elastomer "A" containing "C" phr of nanofiller of type "B."

A Brucker Equinox55 Fourier transform infrared spectrometer (FTIR) was used in the range of 500–4000 cm^{-1} (16 scans per sample) with a resolution of 4 cm^{-1} to investigate surface modification of eggshell powders. To specify curing characteristics like the maximum (M_H) and minimum (M_L) torque values, scorch time (t_2), and optimum cure time (t_{90}), a R100 Monsanto rheometer was used in accordance with ASTM D-2084. The mechanical data consisting of elongation at break and tensile strength were collected by using a 20-kN Zwick apparatus, according to ASTM D-412. The hardness and resilience values of vulcanizates were also measured by using Zwick tester in accordance with ASTM D-2240 and DIN 53512, respectively.

To study the filler–matrix interaction and the degree of filler dispersion throughout the elastomeric matrices, a Philips XL30 SEM was used. Prior to scanning, the cryogenically fractured specimens were gold sputtered. In particular, the thermal stability of SBR nanocomposites from 30 to 600°C was studied by a Shimadzu TGA-50 analyzer at a heating rate of 10°C/min under a nitrogen atmosphere. Moreover, Archimedes principle was used to measure the density of vulcanizates by a Wallace density meter.

RESULTS AND DISCUSSION

Evaluation of Coated Eggshell

The use of an optimal amount of a proper coupling agent ameliorates polymer–filler interfacial interaction.[18] In the current work, FTIR technique is used to witness whether coating of stearic acid onto the surface of eggshell particles was achieved or not. Figure 2 depicts the FTIR spectra of both uncoated and coated eggshell nanoparticles.

Among the several peaks that appeared in modified and unmodified spectra, the ones specified at 3400 and 2514 cm^{-1} are representative for stretching of —N—H and —S—H bonds of cysteine, respectively. This material is a sort of protein that exists in the mammillary layer of eggshell.[19] Moreover, the peaks observed at 1418, 875, and 712 cm^{-1} are proportional to various types of proteins, the stretching of carboxylic groups of amino acids, and the vibration of aromatic —C—H bonds of tyrosine and phenylalanine, respectively. In particular, two distinct peaks are observed at 2916 and 2848 cm^{-1} wave numbers for both modified and unmodified samples. The —C—H stretching of CH_2 groups in unmodified eggshell, spectrum a, is due to eggshell membrane, and the stearic acid coating on eggshell membrane is responsible for more intense peaks of spectrum b at the mentioned wave numbers. As the protein part of mammillary layer of eggshell is not removed while treatment with stearic acid, the triturated AHES is partially coated with stearic acid. Therefore, the peaks observed for modified sample, plot b, are not considerably sharp. In other words, the mentioned peaks of spectrum b witness the contribution of long aliphatic chains of used coupling agent; however, the eggshell membrane makes the peaks more salient. Moreover, physical interaction of nanoparticles with coupling agent agrees with the stronger peak observed at a wave number of 1797 cm^{-1}, proportional to nonadsorbed stearic acid monomers throughout the modified particles.

Table II. Comparison of Mean Particle Size and Specific Surface Area of the Used Fillers

Filler type	Average particle size (nm)	BET area (m^2/g)
CA	50	24.50
AHES	349	8.50

Table III. Compounding Formulation

Ingredient	Loading (phr[a])
Rubber[b]	100
Paraffin wax	2
Zinc oxide	5
Stearic acid	1
Sulfur	1.75
MBTS	0.75
TMTD	1

[a]Parts by weight per 100 parts by weight of rubber, [b]Alternatively NBR, SBR, or NR.

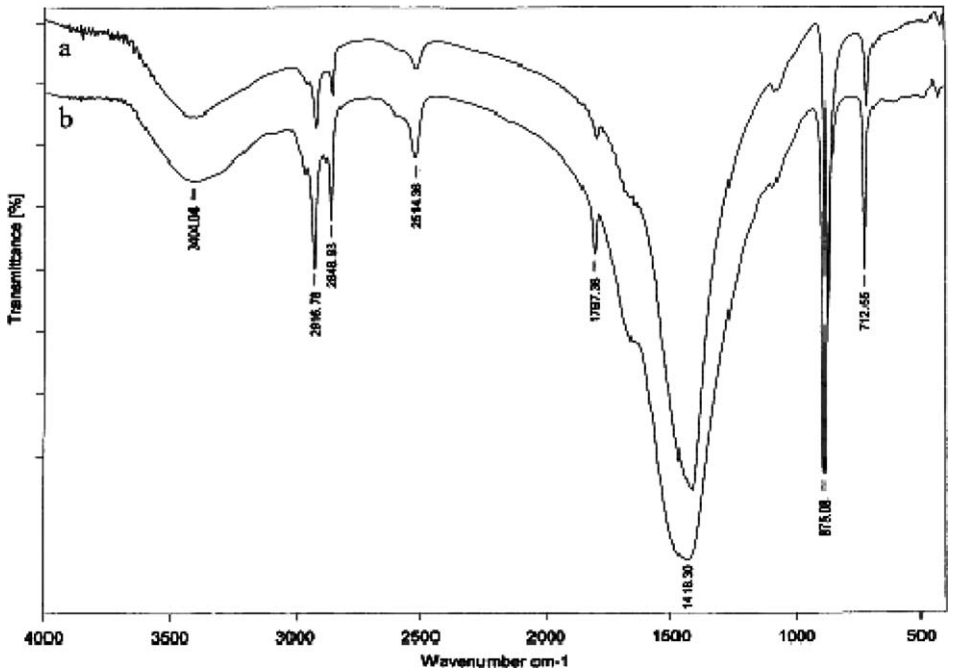

Figure 2. FTIR spectra for eggshell powders: (a) uncoated and (b) stearic acid coated.

Cure Assessment

Figure 3 depicts the difference between maximum torque (M_H) and minimum torque (M_L) values for cured samples as a function of filler content. As seen in this figure, irrespective of the rubber type, the use of eggshell nanofiller reduces the difference between M_H and M_L values (ΔM), particularly at five parts by weight. For NBR nanocomposite, this difference at 5 phr is even lower than that for unfilled compound. On the other hand, all vulcanizates containing CA nanofiller have lower scorch time (t_2) than for those loaded with AHES (Figure 4). It should be noted that the difference between plots representing CA- and AHES-loaded samples is somehow considerable at 5 phr. Nonetheless, adding both types of fillers to unfilled compounds reduces scorch time.

ΔM greatly depends on the degree of crossliking, and hence its increase can be attributed to the increase of the crosslink density. The scorch time decrease may be due to restriction of the mobility of rubber chains occluded by nanoparticles. Figure 5 depicts alteration of optimum cure time for all prepared nanocomposites as a function of loading level. As discussed in the introductory paragraph, the nature of base rubber can highly affect the curing behavior.

NBR is a polar rubber, whereas NR and SBR are not. Therefore, the filler–polymer interaction of AHES particles with NBR

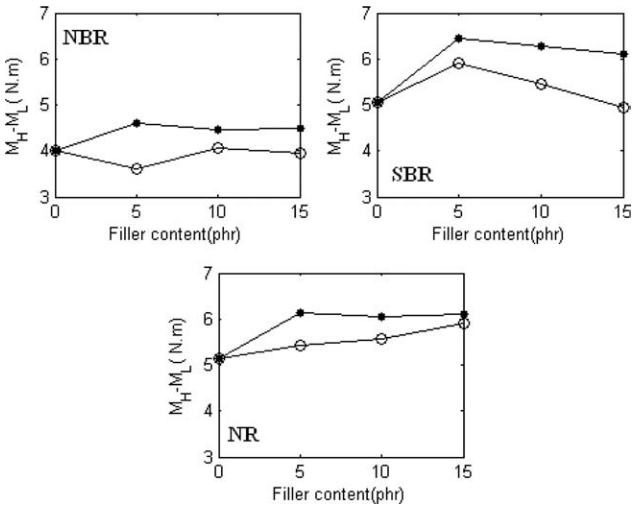

Figure 3. Difference between maximum torque (M_H) and minimum torque (M_L) values of various nanocomposites as a function of CA (●) and AHES (○) content.

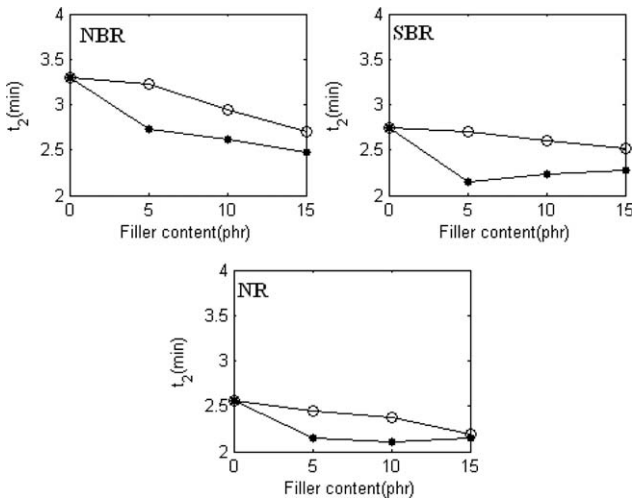

Figure 4. Scorch time (t_2) of various nanocomposites as a function of CA (●) and AHES (○) content.

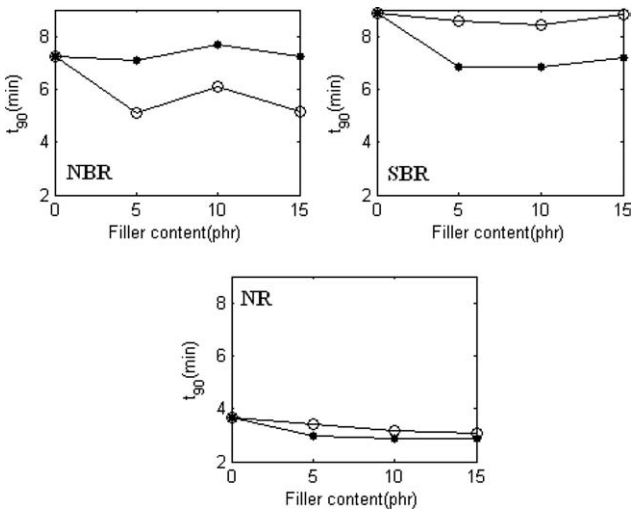

Figure 5. Optimum cure time (t_{90}) of various nanocomposites as a function of CA (●) and AHES (○) content.

rubber is completely different than NR and SBR compounds. Thus, the optimum cure time (t_{90}) of NBR nanocomposite is reduced while using AHES instead of CA, whereas inverse trends are observed in plots of NR and SBR nanocomposites. This contradictive behavior has already been observed regarded to optimum cure time of the same elastomeric systems consisting of micron-sized CA and AHES.[17] Hence, the effects of the type of nanofiller and rubber have to be simultaneously considered. The change in crosslink density and crosslink type can also be considered because the organic part of AHES (mainly amino acids) probably plays a major role in curing efficiency.

Crosslink Density Measurement

Ultimate properties of cured systems highly depend on curing condition. Moreover, the addition of nanofillers in rubber compounds results in a change in filler–polymer interfacial energy leading to further crosslink density of vulcanizates. Nonetheless, reducing the average number of intermolecular bonds per unit volume on account of the structural changes in polymer–solid adhesion and also lowering the packing density of the polymer chains are other probable circumstances. Ignoring the effect of filler–matrix interactions, all cured samples are swollen by toluene to calculate the crosslink density through Flory–Rehner equation[20]:

$$n = \frac{-[\ln(1-\upsilon_2)+\upsilon_2+\chi_1\upsilon_2^2]}{V_1(\upsilon_2^{1/3}-\upsilon_2/2)}, \quad (1)$$

where n is the crosslink density, V_1 is the molar volume of used solvent (106.28 cm^3/mol), υ_2 is the volume fraction of polymer in the swollen sample, and χ_1 stands for the Flory–Huggins polymer–solvent interaction parameter or the enthalpy of mixing, which can be found in the literature[20] or determined by the following equation:

$$\chi_1 = \beta_1 + \frac{V_1(\delta_1-\delta_2)^2}{RT}, \quad (2)$$

where β_1 is lattice constant of entropic origin and is often assumed to be zero, T is the medium temperature, δ_1 and δ_2 are solubility parameters for solvent (18.2 $MPa^{0.5}$ for toluene) and polymer (20.26 $MPa^{0.5}$ for NBR, 17.39 $MPa^{0.5}$ for SBR, and 16.69 $MPa^{0.5}$ for NR), respectively.[21,22]

Elsewhere, Marzocca[23] has found the following relation between the polymer volume fraction at equilibrium (maximum) degree of swelling and Flory–Huggins polymer–solvent interaction parameter:

$$\chi = 0.524 - 0.285\upsilon_2. \quad (3)$$

In eq. (3), the amount of υ_2 can be calculated from the following equation:

$$\upsilon_2 = \frac{1}{1+SR(\rho_2/\rho_1)}, \quad (4)$$

where SR is the equilibrium swelling ratio of vulcanized sample, ρ_2 is its density, and ρ_1 is the density of the solvent (0.8669 g/cm^3). In the filled systems, υ_2 is a bit different from the value calculated using the above equation. Using the above-mentioned relations, the crosslink density of all nanocomposites are calculated and then plotted in Figure 6.

The nanosized, uniformly distributed, and dispersed filler takes up more volume, forcing the polymer and curing agents in a smaller space making the reactions more probable and thus enhancing the crosslinking.[5] At higher loading levels, however, the decline in crosslink density is expected due to aggregated particles. This trend is entirely observed in the plots of Figure 6, irrespective of the type of rubber. Furthermore, irrespective of the type of base rubber and filler content, compounds containing AHES particles have lesser crosslink densities. These observations are in good agreement with alteration of ΔM, as discussed in "Cure Assessment" section.

Another aspect of Figure 6 is the influence of the type of rubber used. As the solubility parameter of NBR compound is quite

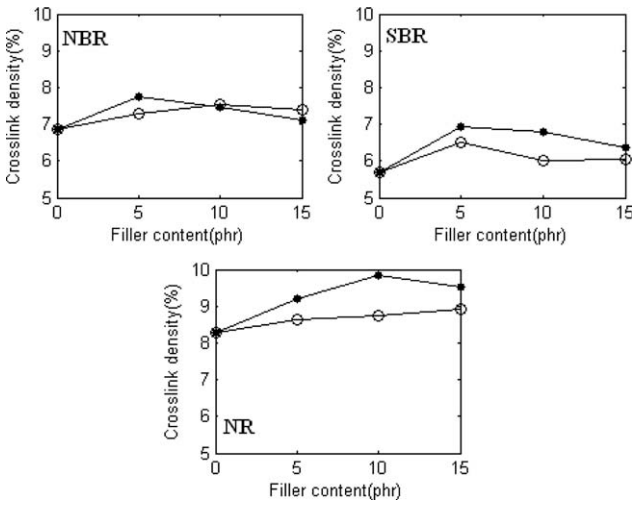

Figure 6. Crosslink densities calculated for various nanocomposites as a function of CA (●) and AHES (○) content.

Table IV. Physical and Mechanical Properties of the Vulcanizates

Sample	100% modulus (N/mm^2)	200% modulus (N/mm^2)	300% modulus (N/mm^2)	Hardness (shore A)	Resilience (%)	Density (g/cm^3)
NBR/CA/5	0.82 ± 0.04	1.19 ± 0.05	1.40 ± 0.03	56 ± 2	46 ± 1	1.070
NBR/CA/10	0.85 ± 0.04	1.24 ± 0.04	1.47 ± 0.05	60 ± 3	44 ± 1	1.095
NBR/CA/15	0.84 ± 0.01	1.23 ± 0.04	1.45 ± 0.05	59 ± 4	43 ± 1	1.130
NBR/AHES/5	0.74 ± 0.05	1.12 ± 0.02	1.34 ± 0.02	57 ± 4	45 ± 1	1.080
NBR/AHES/10	0.82 ± 0.06	1.20 ± 0.02	1.44 ± 0.02	59 ± 1	47 ± 1	1.095
NBR/AHES/15	0.85 ± 0.05	1.24 ± 0.04	1.46 ± 0.02	59 ± 0	45 ± 0	1.115
SBR/CA/5	-	-	-	56 ± 1	71 ± 1	1.040
SBR/CA/10	1.32 ± 0.01	-	-	55 ± 2	70 ± 1	1.055
SBR/CA/15	1.32 ± 0.08	-	-	55 ± 2	68 ± 1	1.100
SBR/AHES/5	1.30 ± 0.03	-	-	55 ± 4	70 ± 1	1.025
SBR/AHES/10	1.30 ± 0.06	-	-	55 ± 1	68 ± 1	1.060
SBR/AHES/15	1.27 ± 0.03	-	-	55 ± 4	69 ± 1	1.080
NR/CA/5	1.23 ± 0.01	2.33 ± 0.06	3.74 ± 0.09	48 ± 2	78 ± 1	0.995
NR/CA/10	1.29 ± 0.02	2.43 ± 0.04	3.91 ± 0.04	50 ± 2	78 ± 1	1.020
NR/CA/15	1.37 ± 0.04	2.57 ± 0.03	4.09 ± 0.06	50 ± 1	78 ± 2	1.045
NR/AHES/5	1.11 ± 0.06	1.95 ± 0.06	3.07 ± 0.25	49 ± 1	79 ± 1	1.000
NR/AHES/10	1.15 ± 0.06	2.02 ± 0.13	3.18 ± 0.07	48 ± 2	79 ± 1	1.015
NR/AHES/15	1.20 ± 0.06	2.14 ± 0.05	3.37 ± 0.08	48 ± 5	78 ± 1	1.035

different with that of toluene, the crosslink density alteration in not dependent on the filler type. On the other hand, AHES and CA nanoparticles have different effects on crosslink density of SBR and NR nanocomposites. In a general sense, there are two theoretical explanations for swelling behavior of the filled polymers: (1) solvent disturbs the interactions between polymer chains and filler surfaces so that breakage of many of bonds at the interface may occur, and 2) polymer–filler bonds remain unaffected, completely or partially, in the presence of the solvent. In the case of the complete breakdown of interface bonds, there is a significant rise in the apparent swelling of rubber; hence, the difference between filler and matrix interactions can be misleading in the calculation of crosslink density.[23]

Physical and Mechanical Properties

Table IV represents some physical and mechanical properties of the prepared nanocomposites. Generally, when filler content increases, the rubber–filler interaction increases, which causes the increase of hardness, tensile strength, and modulus. According to Table IV, the use of CA nanofiller, when compared with AHES, results in slight improvement of modulus. The NBR nanocomposites containing 15 phr of AHES and CA, however,

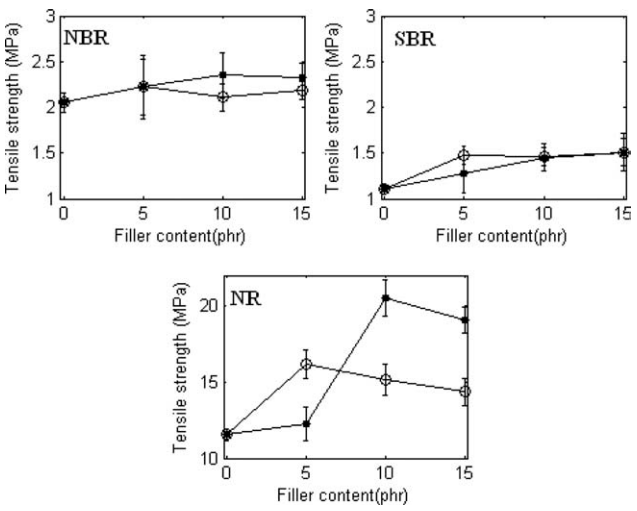

Figure 7. Tensile strength of various nanocomposites as a function of CA (●) and AHES (○) content.

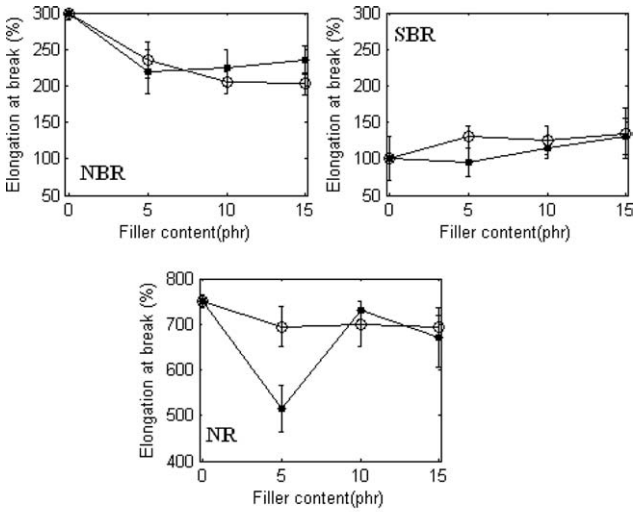

Figure 8. Elongation at break of various nanocomposites as a function of CA (●) and AHES (○) content.

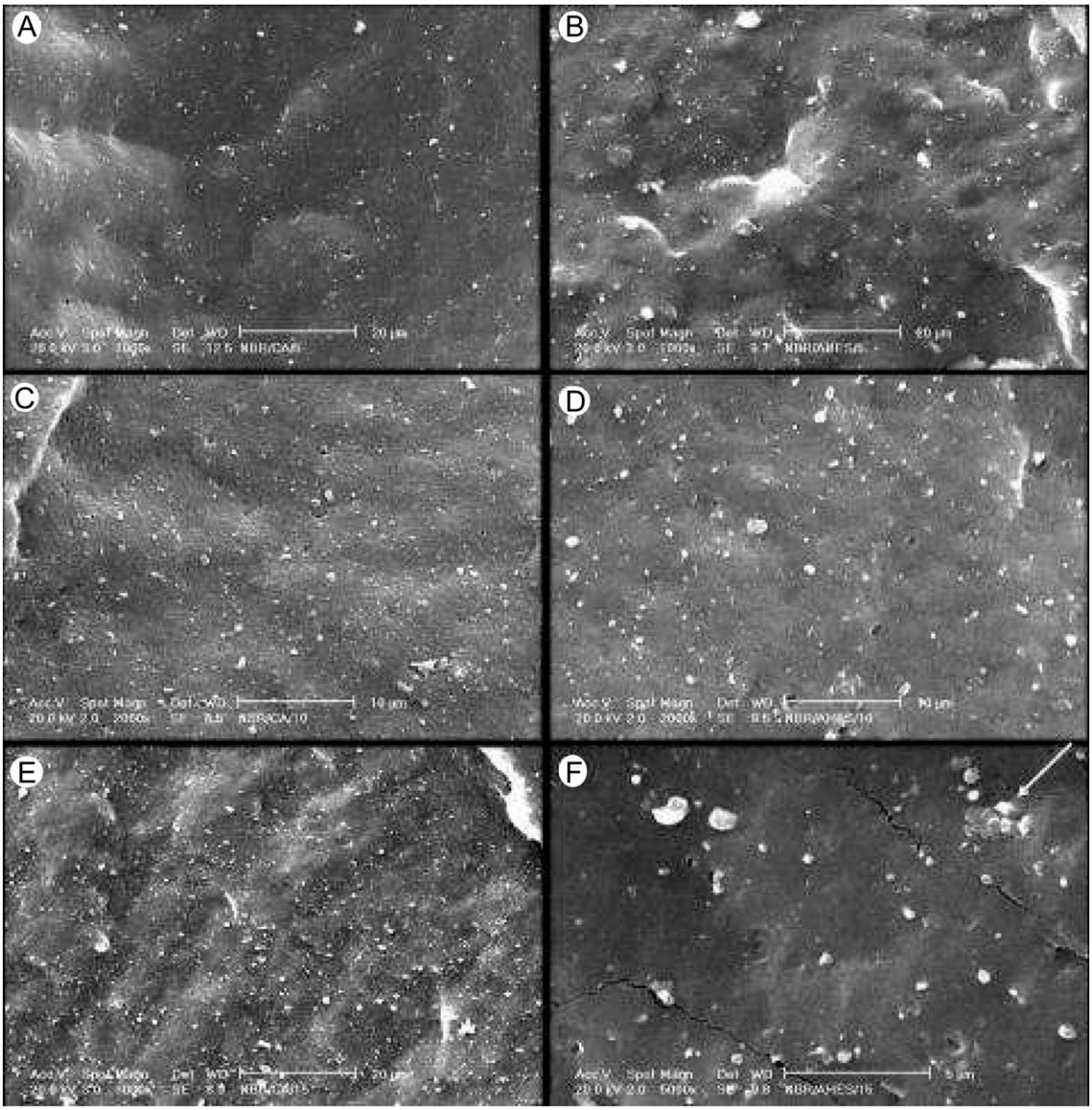

Figure 9. SEM images of NBR nanocomposites: (A) NBR/CA/5; (B) NBR/AHES/5; (C) NBR/CA/10; (D) NBR/AHES/10; (E) NBR/CA/15; and (F) NBR/AHES/15.

have almost equal tensile modulus. An increase in the tensile modulus of polymer composites is always expectable while reducing the particle size of particulate fillers.[13] Despite the fact that the average size of AHES particle is more than that of CA (Table II), the tensile modulus is not highly dependent on the type of filler. It is also noted that the modulus of eggshell is lower than that of limestone and marble; nevertheless, they almost have the same ingredients in them.[19]

Thus, good dispersion of the filler throughout the rubber, which increases the interfacial bonding between polymer and nanofiller, should be considered as well. This fact reasons partial improvement of modulus for CA-based nanocomposites. Nevertheless, the consequence of the nature of elastomer used can also be taken into account.[7,11]

The increase in hardness is not observed with the addition of both types of nanofillers. This unexpected behavior can be attributed to agglomeration with higher concentrations and to the poor filler–polymer interactions. Furthermore, a slight decrease in resilience was expected due to the restriction of the rubber chains mobility resulting from the physical crosslinks introduced by the nanofiller. As the values for densities are somehow independent of the kind of filler used (Table IV), the hypothesis of poor filler–polymer interaction would be reasonable.

Figure 7 shows tensile strength against filler content for all types of nanocomposites. Customarily, tensile strength of vulcanized rubber roughly increases when a small part of crosslink forms

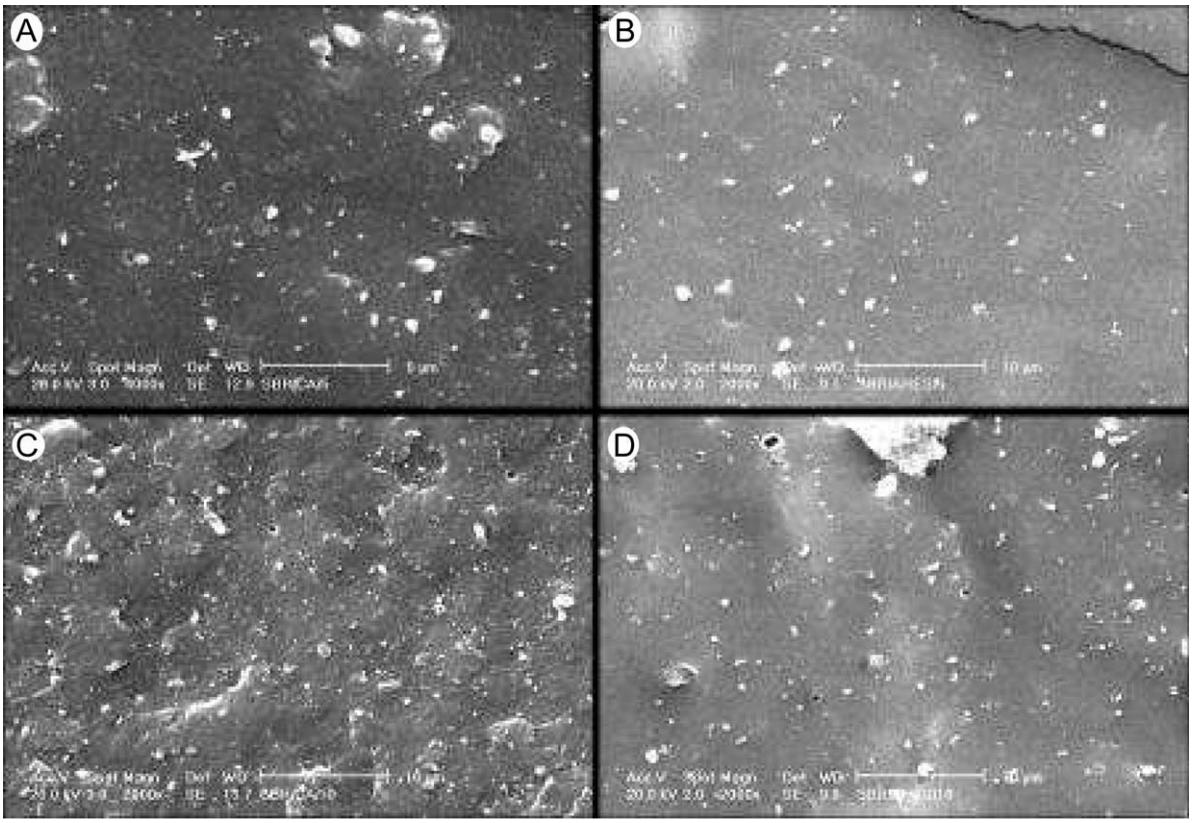

Figure 10. SEM images of SBR nanocomposites: (A) SBR/CA/5; (B) SBR/AHES/5; (C) SBR/CA/10; and (D) SBR/AHES/10.

throughout rubber compounds, whereas it lowers by further crosslink formation. In other words, tensile strength undergoes an optimum at some intermediate crosslink density.[5,24] This type of behavior is observed in Figure 7 for all types of rubbers containing either AHES or CA nanofillers. However, the optimum occurs at a filler content of 10 phr for CA-loaded compounds, whereas for AHES-loaded compounds, it occurs at 5 phr. Moreover, among all elastomeric nanocomposites, the tensile strength of NR compound highly depends on the type of used filler. An inverse trend was already seen for optimum cure time of NR nanocomposites (Figure 5). Hence, AHES and CA interact with NR rubber chains in different ways. The mean particles size of AHES is about seven times of that for CA, which may cause this difference in tensile strength of NR with NBR and SBR nanocomposites. Moreover, because of the surface roughness of AHES, this biofiller at low contents can easily interact with flexible chains of NA leading to increase in tensile strength. This increase is limited in the case of SBR nanocomposites at assigned loading level. On the other hand, at higher filler contents, higher degree of interfacial adhesion on account of lesser agglomerates in CA-filled compounds results in higher tensile strength. This hypothesis is proven in the next section based on SEM micrographs corroborating the role of particle size of CA at higher loading levels. The analysis of elongation at

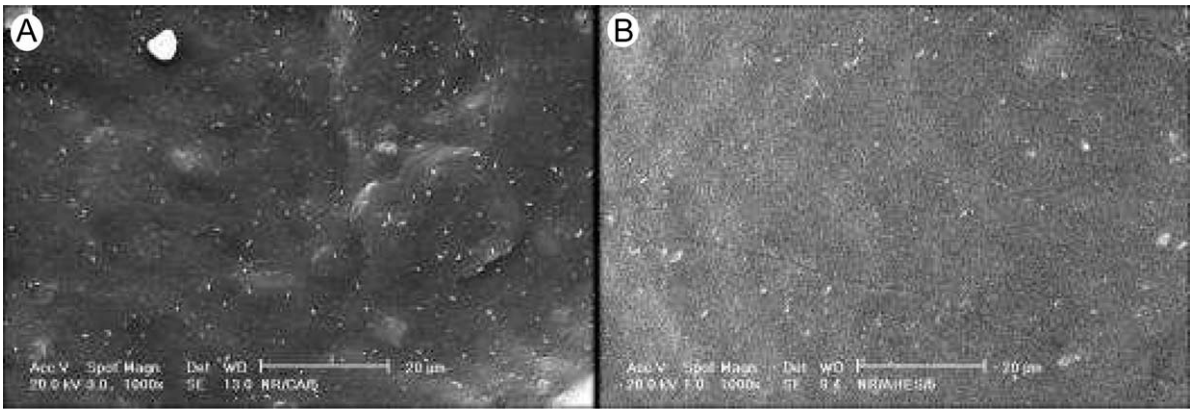

Figure 11. SEM images of NR nanocomposites: (A) NR/CA/5 and (B) NR/AHES/5.

Table V. Thermal Stability Factors of SBR-Based Nanocomposites Obtained from TGA

	SBR/CA/5	SBR/CA/10	SBR/CA/15	SBR/AHES/5	SBR/AHES/10	SBR/AHES/15
IDT	423.38	424.39	423.27	425.34	422.51	424.88
T_{max}	439.48	441.98	442.94	442.74	439.76	440.48
Char content at 590°C (%)	17.54	19.38	21.68	16.95	19.97	23.47

break in Figure 8 demonstrates similar trend regarding to filler type and content. A drop in elongation at break can be seen for the filled compounds, particularly while using CA nanofiller, because of the decrease of the rubber content in the matrix with respect to unfilled compounds.

Morphological Analysis

For better understanding of the alteration of mechanical properties in the filled systems, the dispersion and distribution of filler within polymer matrix need to be studied. The polymer–filler interaction, which highly depends on filler shape, particle size, and distribution, determines the amount of agglomerates in the nanocomposite.[4,5,7,24] The SEM pictures of the NBR, SBR, and NR nanocomposites are given in Figures 9–11.

In NBR compounds, the distribution of AHES and CA in the matrix is roughly the same at low filler content of 5 phr [Figure 9(A, B)]. With increasing filler content, agglomerates and aggregates of the AHES particles are visible as small white spots on the background [Figure 9(F)] and likewise for SBR nanocomposites (Figure 10). Despite the fact that CA nanofiller has smaller particle size than that of AHES, most viewed properties at low filler content are better while using AHES biofiller. The behavior of nanoparticles can be determined by the modification agent and by the chemical nature of the filler. The polar accelerators can be adsorbed onto the polar filler surface, which leads to retardation of the vulcanization process. When AHES is added to NBR compound, curing is faster when compared with the CA-filled compounds. This is partly caused by high probability of crossliking reaction due to porosity of AHES particles, which reasons higher mechanical properties at 5 phr loading. At higher contents, however, AHES nanoparticles are very potent to form aggregates, which results in stress concentration and declines the tensile properties. In contrast, the higher interfacial area is achieved when small CA particles are added to the elastomers. Therefore, the role of particle size for CA and porosity for AHES fillers seems to be important. It should be noted that the results of this study were more complex than those reported in the literature. It is possible that the high amount of used fillers in addition to the special type of AHES biofiller prevented the system to be cured properly.

Thermal Properties of the SBR Nanocomposites

The SBR nanocomposites are particularly considered for measuring the thermal stability. Table V represents thermal stability parameters consisting of the initial decomposing temperature (IDT), the temperature at maximum rate of weight loss (T_{max}), and char content at 590°C (%) for SBR/CA and SBR/AHES nanocomposites prepared in the current work.

Moreover, decomposition behavior of these systems is plotted in Figure 12. Accordingly, the AHES had only a minor effect on the thermal stability of SBR compound when compared with CA nanoparticles. Nonetheless, with increasing filler content, the T_{max} is reduced in AHES nanoparticles. Similar trend was observed for SBR/CA nanocompounds while using smaller nanofillers in SBR/CA[5] and also in butadiene rubber/CA nanocomposites.[4] The char content at 590°C, however, alters in a narrower range (17.54–21.68) for CA-filled compounds with increasing filler content. More char content at high loading levels supports the existence of organic ingredients in the AHES biofiller.

CONCLUSION

This study compares the effect of using two alternative nanofillers, hatched eggshell (AHES) and CA, on the mechanical and cure characteristics of NR, NBR, and SBR nanocomposites. It is

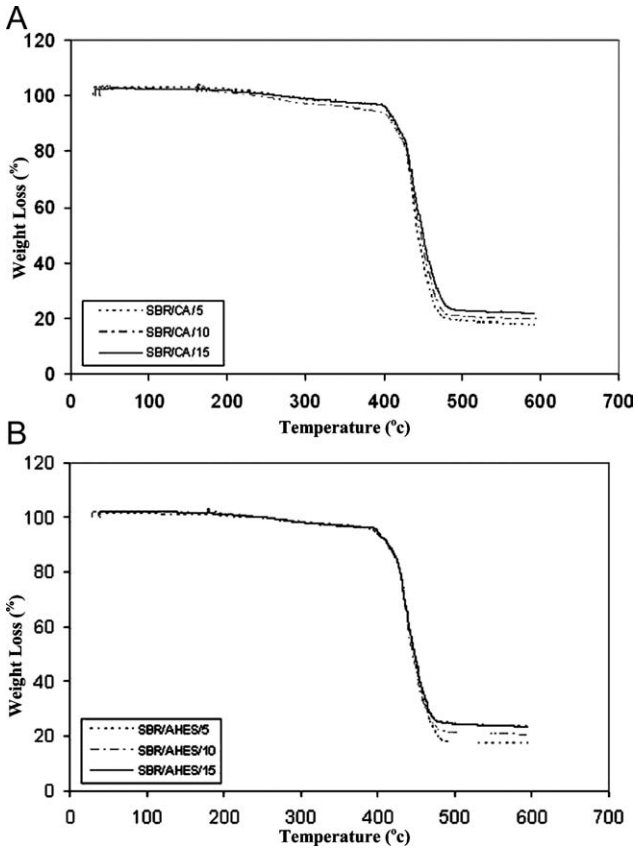

Figure 12. Weight loss percent as a function of temperature for (A) CA/SBR and (B) AHES/SBR nanocompounds.

found that the mentioned properties change by the type of filler, loading content, and somehow by the nature of elastomer. At low loading levels (5 phr), AHES-filled compounds show better properties rather than CA-filled nanocomposites, whereas CA can contribute to improve ultimate properties at higher contents. The reason is that AHES has porous structure that provides better filler–polymer interaction at low contents. The CA particles are seven times smaller than that of AHES, which results in better dispersion at higher loading levels, whereas AHES is very potent to form as agglomerate. NBR nanocompounds are not affected by the type of filler used, which can be due to the limited movement of NBR chains while using mineral and natural fillers. Eventually, thermogravimetric analysis showed similar thermal stability for SBR nanocomposites containing AHES and CA fillers.

REFERENCES

1. Morton, M. In Rubber Technology; Morton, M., Ed.; Van Nostrand Reinhold Company: New York, **1987;** Chapter 1, p 10.
2. Osman, M. A.; Atallah, A.; Suter, U. W. Polymer **2004,** *45*, 1177.
3. Sahebian, S.; Zebarjad, S. M.; Sajjadi, S. A.; Sherafat, Z.; Lazzeri, A. *J. Appl Polym. Sci.* **2007,** *104*, 3688.
4. Jin, F.-L.; Park, S.-J. *Mater. Sci. Eng. A.* **2008,** *478*, 406.
5. Mishra, S.; Shimpi, N. G.; Patil, U. D. *J. Polym. Res.* **2007,** *14*, 449.
6. Zhang, H.; Chen, J. F.; Zhou, H. K.; Wang, G. Q.; Yun, J. *J. Mater. Sci. Lett.* **2002,** *21*, 1305.
7. Yang, K.; Yang, Q.; Li, G.; Sun, Y.; Feng, D. *Polym. Compos.* **2006,** *27*, 443.
8. Xu, X.; Song, Y.; Zheng, Q.; Hu, G. *J. Appl. Polym. Sci.* **2007,** *103*, 2027.
9. Jiang, L.; Lama, Y. C.; Tam, K. C.; Chua, T. H.; Sim, G. W.; Ang, L. S. *Polymer* **2005,** *46*, 243.
10. Lipińska, M.; Zaborski, M.; Ślusarski, L. *Macromol. Symp.* **2003,** *194*, 287.
11. Mnif, N.; Massardier-Nageotte, V.; Kallel, T.; Elleuch, B. *Int. J. Mater. Form.* **2008,** *1*, 639.
12. Zhou, Y.; Wang, S.; Zhang, Y.; Jiang, X.; Yi, D. *J. Appl. Polym. Sci.* **2006,** *101*, 3395.
13. Toro, P.; Quijada, R.; Yazdani-Pedram, M.; Arias, J. L. *Mater. Lett.* **2007,** *61*, 4347.
14. Zurale, M. M.; Bhide, S. *J. Mech. Compos. Mater.* **1998,** *34*, 463.
15. Kang, D. J.; Pal, K.; Park, S. J.; Bang, D. S.; Kim, J. K. *Mater. Des.* **2010,** *31*, 2216.
16. Ramezani-Dakhel, H.; Heshmati, V.; Saeb, M. R. In Proceedings of the 7th International Conference on Composite Science and Technology, Sharja, UAE, January 20–22, **2009.**
17. Ramezani-Dakhel, H. *e-Polymers* **2008,** *140*, 1618.
18. Wan, W.; Yu, D.; Xie, Y.; Guo, X.; Zhou, W.; Cao, J. *J. Appl. Polym. Sci.* **2006,** *102*, 3480.
19. Solomon, S. E. Egg and Eggshell Quality; Wolfe Publishing: Aylesbury, **1991.**
20. Sperling, L. H. Introduction to Physical Polymer Science, 4th ed.; Wiley: New York, **2006;** Chapter 2, p 74.
21. Grulke, E. A. In Polymer Handbook, 4th ed.; Brandrup, J.; Immergut, E. H.; Grulke, E. A., Eds.; Wiley: New York, **1999;** *Vol.* 2, p 675.
22. Wang, S. In Polymer Data Handbook; Mark, J. E., Ed.; Oxford University Press: Oxford, **1998;** p 1.
23. Marzocca, A. J. *Eur. Polym. J.* **2007,** *43*, 2682.
24. Xu, Y.; Hanna, M. *Packag. Sci. Technol.* **2007,** *20*, 165.